Design of 3D Printed Below-Knee Prosthetic -
A Finite Element and Topology Optimization Study

Ozbil Ozmen[1] – Hasan Kemal Surmen[2,*]

[1] Istanbul Okan University, Department of Machine and Metal Technologies, Turkey
[2] Istanbul University-Cerrahpasa, Department of Motor Vehicles and Transportation Technologies, Turkey

There are approximately 35 to 40 million people worldwide who require assistive devices, including prosthetics and orthoses. Most amputee patients have a lower amputation. The high cost of prosthetics, long production and delivery times, the frequent need for prosthetics in growing children and limited accessibility to prosthetics are common complaints of amputees. This study aims to design and fabricate a lightweight, high-strength, low-cost and easily accessible three dimensional (3D) printed below-knee prosthetic leg without support material to improve the quality of life of amputees. First, a flexible and jointless one-piece below-knee prosthetic leg model was designed by considering the anthropometric data of children who frequently require prosthetics. Then, using the finite element and topology optimization methods, an optimized prosthetic leg model was developed according to the results of structural analyses performed by considering the loading conditions and boundary conditions during daily activities such as standing, walking, ascending and descending stairs. Finally, the prosthetic model was modified for a support-free additive manufacturing process and a socket and heel piece were added. The designed prosthetic leg model was fabricated using the additive manufacturing method with hard thermoplastic polyurethane (TPU) material. The final prosthetic leg design achieved a safety factor of 4.14 and a weight reduction of 50.37 % compared to the solid model. In addition, a 50 % reduction in material usage and a 32 % reduction in fabrication time were achieved through topology optimization and support-free design.
Keywords: 3D printing, additive manufacturing, FEM, prosthetic design, topology optimization

Highlights
- *An optimized below-knee prosthetic was improved for the conditions of standing, walking, stair ascending and descending.*
- *Additive manufacturing was employed to fabricate the optimized and support-free prosthetic design with complex geometry.*
- *The weight of the prosthetic was reduced by 50.37 % using the topology optimization method.*

0 INTRODUCTION

Medical procedures such as prosthetics are used to increase the quality of life of amputee patients and to enable them to reclaim their social life. Prosthetics are artificial devices that are used to replace a missing body part [1]. Prosthetics are designed to improve the quality of life by focusing on the needs of amputees. Lower limb prosthetic systems can be considered in four categories, taking into account user needs such as physical, psychological, ergonomic and other needs of amputees [2]. Physical needs in this study reflect the requirements for the user to be able to perform physical activities such as standing, walking, ascending and descending stairs. Ergonomic needs reflect requirements such as ease of use, comfort, lightness of weight and reduced perspiration. In addition, durability, wearability, low cost, and easy accessibility are other needs reported by users. The aim of this study was to develop a prosthetic leg design that incorporates these features, taking into account the user needs of amputees, and to produce it using an additive manufacturing process, i.e. three-dimensional (3D) printing.

The first 3D prosthetic leg model was designed in computer-aided design (CAD) software considering the anthropometric data of the children that are given in the study by Ocak and Gulumser [3] and the design method in the study by Tao et al. [4]. The design of the prosthetic was based on the need for the prosthetic model to be strong enough to safely withstand the loads, while at the same time achieving a lightweight prosthetic to reduce the load on the existing muscles in order to improve the amputee's quality of life. According to the study conducted by Preatoni et al. [5], it is understood that amputees perceive that the prosthetic feels heavier even when the weight of the prosthetic leg and the weight of the limb are the same. As a result of these amputee complaints, the aim was for the weight of the prosthetic to be lighter than the weight of the limb. Therefore, topology optimization analysis was used to design a lightweight and durable prosthetic leg. In addition, topology optimization reduces material consumption and production time. Structural topology optimization designs have become one of the most important tools to achieve low-cost, lightweight and high strength products. Topology optimization is the optimal design approach that can be achieved at the lowest cost within the operational

*Corr. Author's Address: Istanbul University-Cerrahpasa, Department of Mechanical Engineering, Turkey, hksurmen@iuc.edu.tr

517

performance and capabilities [6]. Therefore, the finite element method (FEM) has been used effectively [7] to [10]. Recently, there has been a growing interest in applying computational methods such as FEM in the development of biomedical devices such as prosthetics, orthoses and implants [11] and [12]. In the present study, the structural analysis of the first designed 3D prosthetic leg model was performed using FEM in ANSYS Workbench software by investigating the loading conditions such as standing, walking, ascending stairs, and descending. Later, the analysis results were compared according to the loading conditions.

The topology optimization analysis was carried out by evaluating the stresses obtained as a result of the analysis. The aim of the study was to produce a prosthetic design lighter than the actual limb weight, such that it corresponds to 5.7 % of the body weight, as suggested by the study by de Leva [13]. In addition, a socket section designed for sweatless easy wear has been added to the existing design. Later, a heel section was added to facilitate the wearing of shoes and to ensure better balance. Since the optimized designs have complex geometries and free forms, they are well suited to the additive manufacturing methods, which allow a direct transition from design to production and the production of parts with complex geometries [14]. In addition, the use of 3D printers can provide prosthetics with an online connection for fabrication in many parts of the world where prosthetic production and supply is geographically inaccessible.

Metals, ceramics, plastics and composites are used as prosthetic materials [15]. As a polymer prosthetic is lighter and less costly than a prosthetic made of other materials, a polymer material, hard thermoplastic polyurethane (TPU) was preferred in this study. TPU is known for its high-strength, flexibility and non-slip features [16] and [17]. Fused deposition modeling (FDM) was used to fabricate the prosthetic. FDM is the most commonly used additive manufacturing method for the production of polymer material parts [18]. Some 3D printing technologies, such as FDM [19], need support structures when printing of slopes greater than 45 degrees [20]. Support structures are removed from the product after printing by mechanical or chemical methods. This process wastes time, labour and material and increases the cost of the product [20] and [21]. In this study, the design of the prosthetic leg was modified after the optimization process, taking into account the 45-degree rule, so that the support structure was not required.

Finally, the design and production of the novel low-cost prosthetic leg with a 3D printer, which is lightweight and optimized to meet the loads that may occur during use, are discussed and evaluated in this study.

1 MODELS AND METHODS

The first 3D prosthetic leg model was designed in one piece, taking into account the average foot anthropometry of children, a patient group that often requires frequent prosthetic replacement [3].
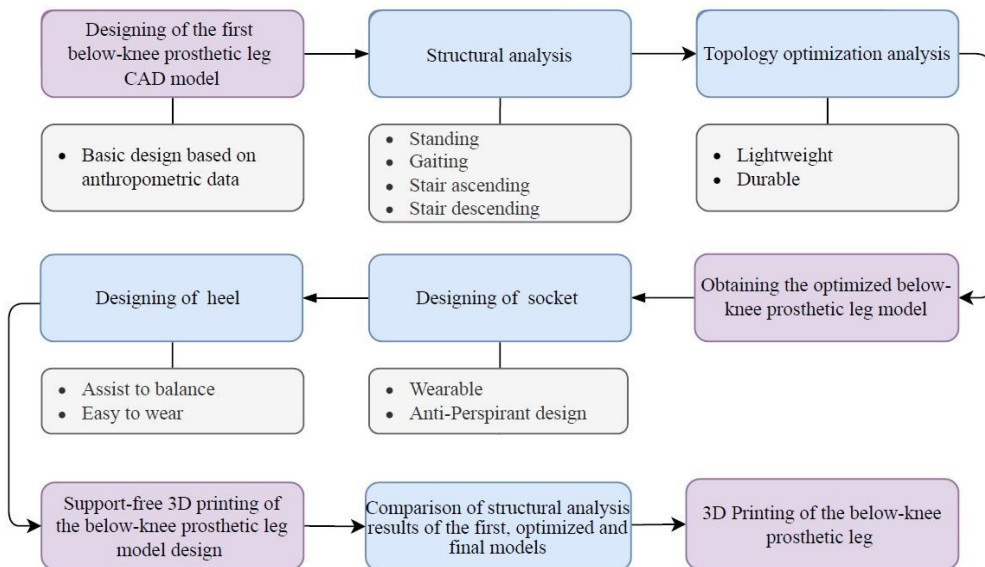

Fig. 1. *Workflow of the design and manufacturing of the below-knee prosthetic leg*

Stress and deformation results were obtained from structural analyses using the finite element method. The loading conditions were determined according to the daily activities of the lower limb amputees, such as standing, walking, ascending and descending stairs. The average weight was taken as 220 N in the calculation of the applied force for the FEM analysis [3].

The optimized model of the prosthetic was obtained by performing topology optimization analysis in the Ansys Workbench software. The highest stress value obtained from the structural analysis results was used as the loading condition in the topology optimization analysis.

Later, a socket section for wearing the prosthetic and a heel section for better balance were designed and added to the prosthetic design.

The final below-knee prosthetic leg model was designed for a support free 3D printing process. Structural analysis of the final model was performed to compare the first and optimized prosthetic models in terms of lightness, safety factor, stress and deformation. The final model was manufactured in a 3D printer using FDM technology and TPU material. The workflow diagram of the design and manufacturing process of the below-knee prosthetic leg is shown in Fig. 1.

1.1 Design of the First 3D Model of the Below-Knee Prosthetic Leg

The first 3D model of the below-knee prosthetic leg was designed as a single piece without joints, taking into account the anthropometric data of foot length, foot width, heel width and ankle circumference of 69 boys in the study by Ocak and Gulumser [3]. According to these data, a 3D model of this primitive model of the prosthetic leg was designed in CAD software, as shown in Fig. 2. This 3D model is the basic model before optimizations.

1.2 Boundary Conditions and Parameters

The loading conditions of the amputee patient during standing, walking, ascending and descending stairs were investigated during the design improvement of the below-knee prosthetic leg. The foot is a limb that provides balance, carrying body weight safely, and propels the body forward during movement [22]. The ground responds to the force exerted by a person standing on it with an opposite force of the same magnitude, according to Newton's third law, also known as the action-reaction law [23]. In the case of

standing, walking, ascending and descending stairs, the vector of the ground reaction force is formed against the combination of body weight and the muscle forces that provide the movement. The direction and magnitude of the ground reaction force change during movement. The amputee's loading conditions during standing, walking, ascending stairs and descending, as well as the direction and magnitude of the ground reaction force, have been considered in the design of the prosthetic.
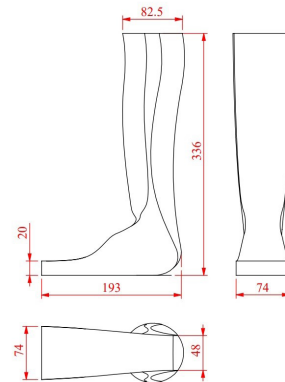

Fig. 2. *Orthographic views of the first CAD model of the below-knee prosthetic leg; all dimensions in mm*
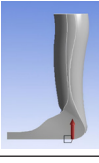
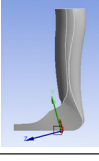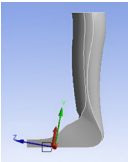In the standing condition, the ground reaction force was taken to be the body weight and a ground reaction force of half the body weight was applied to the single prosthetic leg model in the vertical direction.

In the second condition, the walking movement was investigated. Walking consists of stance and swing phases, and the phase stages [24] were evaluated for our 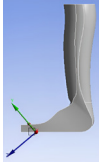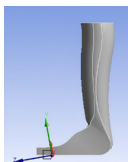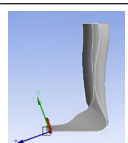study as recorded in Table 1. The gait cycle consists of 60% of the stance phase and 40 % of the swing phase. When both limbs are in contact with the ground during the gait cycle, there is a double support phase, whereas when there is no contact with other limb, there is a single support phase.

The stance phase starts when the foot first touches the ground with the heel strike and ends with the toe-off when the foot no longer touches the ground [25]. The single support phase of the gait cycle occurs during the mid-stance and terminal stance phases, while the double support phase occurs during the other stance phases [24]. Ground reaction forces were applied to the first below-knee prosthetic leg model using plantar flexion and dorsiflexion angles formed at the ankle as the initial contact phase, loading phase, mid-stance phase, terminal phase and pre-swing phase. During the stance phase of the gait cycle, a

ground reaction force equal to half the body weight was applied when a double support phase occurred. When a single support phase occurred, a ground reaction force equal to the body weight was applied. The swing phase was not evaluated in the study as there was no foot contact with the ground during the gait cycle.

Table 1. *Below-knee prosthetic leg loading conditions*

1. Condition Standing	2. Condition Walking	3. Condition Stair ascent/descent	
		Ankle angle	Free body diagram

As a third condition, the ground reaction forces on the prosthetic leg and the angles formed in the amputee's ankle during ascent and descent of the stairs were investigated together.

Protopapadaki et al. [26] determined the functional parameters during stair ascent and descent for healthy humans in their study involving 33 healthy participants and stated the dorsiflexion and plantar flexion angles of the ankle for stair ascent and descent. The angles adapted for our study are shown

in Table 1. Silverman et al. [27] obtained data on the proportion of ground reaction force generated by body weight in a study of 30 participants by examining the ground reaction force data generated during walking, stair ascending and descending. Ground reaction force equal to body weight was applied during walking in this study. According to the data in the study [27], ratios were obtained for plantar flexion and dorsiflexion ankle actions by evaluating the ground reaction force data during stair ascent and descent. These ratios were multiplied by the average weight of 22 kg to obtain the ground reaction forces for stair ascent and descent (Table 2).

Table 2. *Ankle joint angle comparison ratios and forces in stair ascent and descent*

Ankle joint angle	Comparison ratios		Ground reaction forces [N]	
	Stairs ascent	Stairs descent	Stairs ascent	Stairs descent
Plantar flexion	1.01	0.871	222.2	191.6
Dorsiflexion	0.936	1.138	205.9	250.4

1.3 Tensile Strength of 3D Printed TPU Sample

It is planned to 3D print the prosthetic using TPU material. Therefore, a specimen was designed that was suitable for the printing parameters of the prosthetic. The 3D model of the tensile test specimens was designed according to the ASTM D638 TYPE IV dimensions of the ASTM D638 [28] test method, which is used to determine the tensile properties of plastic materials. The 3D model of the designed specimen was transferred to the slicing software. The G-code was generated by adjusting the printing parameters.

Table 3. *Properties of TPU specimen*

Properties	Value
Density [g/cm³]	1.14
Poisson ratio	0.48
Young's modulus [MPa]	360
Tensile yield strength [MPa]	13.33
Tensile ultimate strength [MPa]	26.54

10 specimens were printed for testing. 3D printing parameters of the specimens were also used for the prosthetic leg. All 10 specimens were subjected to tensile testing and the data were averaged to obtain the properties of the TPU specimen shown in Table 3. The data obtained from the mechanical tensile test were

used in the finite element analysis of the prosthetic model.

1.4 Finite Element Analysis

Structural analyses were performed separately using the finite element method on the first 3D below-knee prosthetic leg model for standing, walking, stair ascending and descending conditions by examining the loading conditions of patients with lower amputation. As both feet are in contact with the ground when standing, a ground reaction force of 110 N, half the body weight, was applied to the first model of the prosthetic leg. The direction and angle of the standing force were applied as shown in Table 1.

The initial contact, loading and pre-swing phases of the compression phase of the walking condition constitute a double support phase since both feet are in contact with the ground. A ground reaction force of 110 N, equivalent to half the body weight, was applied during these phases. The mid-stance and terminal stance compression phases of walking form a single support phase because only one foot is in contact with the ground. A ground reaction force of 220 N, equivalent to the body weight, was applied during these phases. The contact zones in the stance phase of walking were indicated in the study by Houglum [24]. The contact zones were adapted to the base of the prosthetic as shown in Fig. 3 of this study. The contact zones at the base of the prosthetics are numbered in the order of initial contact, loading, mid-stance, terminal stance and pre-swing phases. Ground reaction forces were applied to the prosthetic base from the contact zones shown in Fig. 3 and using the ankle angles shown in Table 1. The ankle angles of the dorsiflexion and plantar flexion shown in Table 1 and the ground reaction forces shown in Table 2 were applied for the stair ascending and descending conditions. Structural analyses of standing, walking, ascending and descending stairs were performed in the ANSYS Workbench analysis software and deformation and von Mises stress values were obtained. Since the stresses obtained were below the yield strength, the finite element analysis was performed in the linear region.
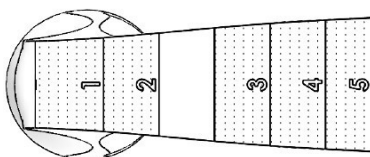

Fig. 3. *Contact zones during walking*

1.5 Topology Optimization Analysis

Patients who have had leg amputation may experience some physical, psychological and ergonomic problems in their daily lives. One of the most important of these problems is the weight of the prosthetic. Prosthetics used by amputees for long periods of time cause more physical fatigue in the prosthetic due to the weight of the body on the prosthetic. There are opinions that the fact that amputees have to move around a lot during the day has a negative impact on energy expenditure, leading to more fatigue and leading to an uncomfortable life [29]. According to the study conducted by Preatoni et al. [5] is understood that amputees perceive that the prosthetic feels heavier even when the weight of the prosthetic leg and the weight of the limb are equal. The weight of the lower extremities corresponds to 5.7 % of body weight according to de Leva's study [13]. The limb weight of the amputee with an average weight of 22 kg is calculated to be 1.25 kg according to this study.

Lightness of weight is one of the primary goals in prosthetic design. A lightweight prosthetic model both improves the quality of life of the amputee patient and reduces the cost of the prosthetic. Thus, the first design of the prosthetic model was optimized aiming at a prosthetic model of less than 1.25 kg with sufficient strength. Structural static analyses were also performed for topology optimization analyses according to the load conditions of standing, walking, ascending stairs and descending conditions and the results were compared and evaluated. While performing the topology optimization analysis, the loading case with the highest stress was taken into consideration. Topology optimization using mathematical programming is known to solve mass reduction problems [30].

$$\sum_{i=1}^{n} \rho_i V_i \leq \bar{M}. \qquad (1)$$

The mass constraint for a structure with n designable finite elements can be shown as shown in Eq. (1). ρ_i in Eq. (1) indicates the material density for element i, which must be interpolated from the set of available material densities. V_i denotes the volume of element i. M is the upper limit that controls the structural mass.

1.6 3D Printing

Conventional methods are difficult to apply to the production of complex models as a result of topology optimization. The additive manufacturing

method, which allows a direct transition from design to production, is suitable for optimized free-form designs. Therefore, there are many studies that use topology optimization and 3D printing together [4] and [21]. In this study, the topology optimization of a below-knee prosthetic leg was performed by the finite element method. After optimization, a 3D model with complex geometry was created, and the 3D printing process is ideal for fabricating this model. In addition, factors such as direct production from design data, fewer staff, low cost and fast supply also make the method suitable for this study. There are several parameters such as print area, print speed, print temperature, plate temperature, fill density, nozzle diameter, layer height, wall thickness, print speed and the use of support material in fabrication with 3D printing. In addition, there is a valid rule known as the 45-degree rule for support structures in 3D printing technologies such as FDM [20].

Table 4. *Printing parameters*

Printing parameters	Value
Layer height [mm]	0.2
Infill line distance [mm]	0.8
Wall thickness [mm]	1.2
Printing temperature [°C]	215
Plate temperature [°C]	60
Print speed [mm/s]	50
Infill density [%]	100

According to this rule, support structures are created for the construction with angles greater than 45-degrees. These structures are then removed when the final product is obtained. The support structures increase both the amount of material and the printing time. It also requires extra labor and time to remove the support structures. In this study, the optimized model was finally modified according to the 45-degree rule for a support-free design. The model was transferred to the slicing software. The pressure parameters determined by the slicing software are shown in Table 4. The final below-knee prosthetic leg model was then printed using an FDM 3D printer.

2 RESULTS

2.1 Results of Structural Static Analysis

Structural static analyses were performed with ANSYS Workbench software using the finite element method in the linear region considering the conditions of the standing, walking, ascending stairs
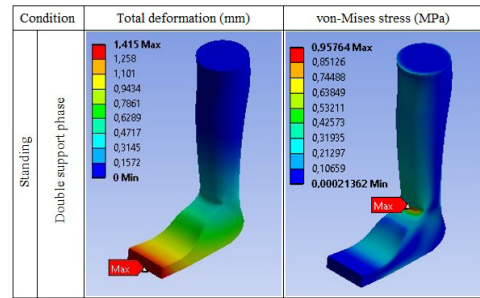

Fig. 4. *Total deformation and stress analysis results according to standing condition*
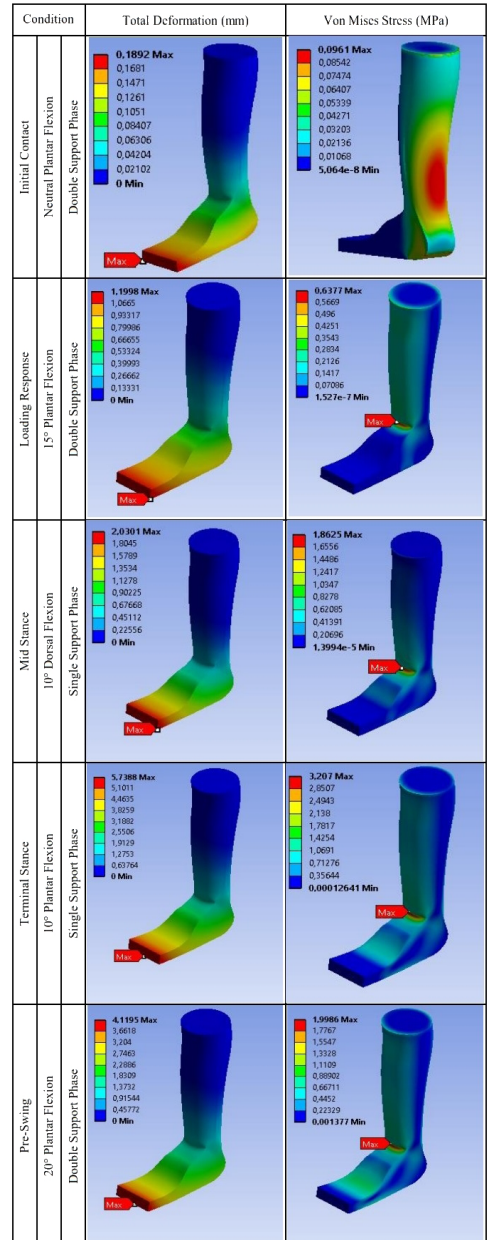

Fig. 5. *Total deformation and stress analysis results of walking condition*
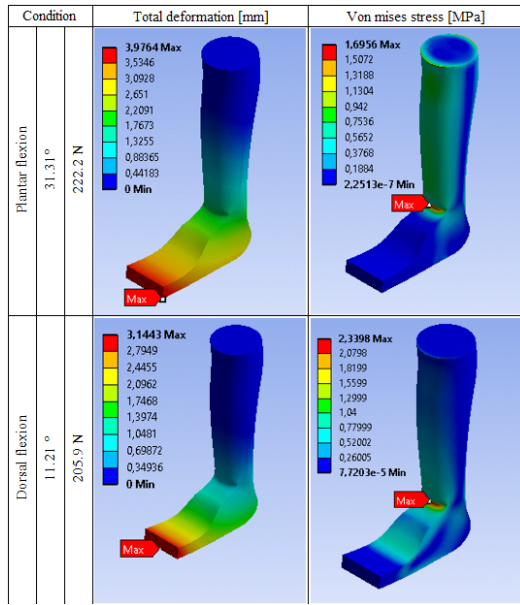
Fig. 6. *Total deformation and stress analysis results at stair ascent condition*

and descending during the daily use of the below-knee prosthetic leg. The results of the total deformation and von Mises stress analyzes for the standing condition are shown in Fig. 4.

The gait cycle consists of the stance and swing phases. Since the loading conditions and contact of the prosthetic with the ground occur during the compression phase, only the compression phase was considered in the finite element analysis. Structural static analyses were performed for the first prosthetic model considering the stance phase stages. The stance phase, which begins with the first contact of the heel with the ground and continues through the loading phase, mid-stance, terminal stance and the

pre-swing phase. Structural analyses were performed considering these phases according to plantar flexion and dorsal flexion angles and single or double support conditions. The results of the total deformation and von Mises stress analysis for the stages of the stance phase are shown in Fig. 5.

For the stair ascent and descent, structural static analyses were performed by considering the plantar flexion and dorsal flexion angles shown in Table 1 and the ground reaction force data shown in Table 2.

The total deformation and von Mises stress analysis results for the stair ascent and descent are shown in Figs. 6 and 8 respectively.

The results of the structural analysis show that the stress in dorsal flexion is higher than the stress in plantar flexion during the stair ascent, and the stress in the plantar flexion is higher than the stress in the dorsal flexion during stair descent. The stress and deformation results obtained from the finite element analyses performed for standing, walking, ascending and descending stairs are evaluated together and shown in Fig. 7. Considering walking, the highest stress in the prosthetic model occurred in the terminal stance phase with 3.207 MPa, while the lowest stress was determined in the initial contact phase with 0.096 MPa. It was observed that the maximum deformation in walking occurred in the terminal stance phase with 5.739 mm, while the minimum deformation occurred in the initial contact phase with 0.189 mm. For the stair ascent and descent, the maximum stress was observed in plantar flexion with 3.009 MPa and the minimum stress was observed in dorsal flexion with 0.84 MPa during the stair descent. The maximum deformation occurred in the plantar flexion with 6.763 mm, while the minimum deformation occurred in
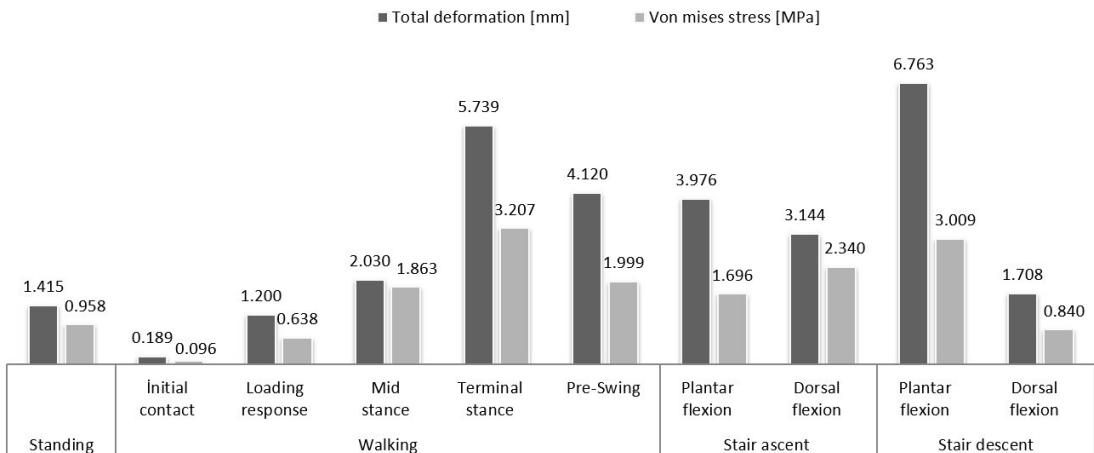

Fig. 7. *Total deformation and stress analysis results according to loading states*

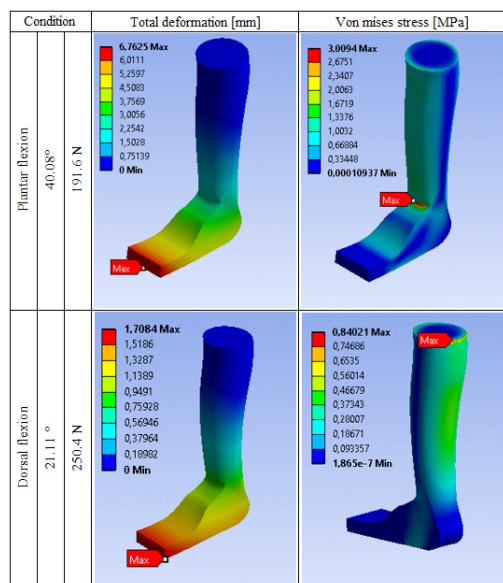the dorsal flexion with 1.708 mm in stair ascent and descent.

Fig. 8. *Total deformation and stress analysis results at stair descent condition*

According to the results of all the analyses for standing, walking, stair ascending and descending conditions; the maximum stress was 3.207 MPa in the terminal stance phase, while the minimum stress was 0.096 MPa in the initial contact phase during walking. According to all loading conditions examined, the highest deformation occurred in the plantar flexion during the stair descent with 6.763 mm, while the lowest deformation occurred in the first contact phase of walking with 0.189 mm.

2.2 Results of Topology Optimization Analysis

As a result of examining the conditions of standing, walking, ascending stairs, and descending stairs, it was determined that the greatest stress in the below-knee prosthetic leg model occurred during the terminal stance phase of walking. A topology optimization analysis was carried out with the aim of designing a prosthetic leg that is lighter than the

weight of the limb, taking into account the maximum load conditions. The weight of the leg below the knee is 5.7 % of the body weight, which is derived from de Leva's study on body anthropometric data [13]. The target population of our study was children with frequent prosthetics needs. Considering the average anthropometric data of the target group, the average weight was determined as 22 kg [3]. In this case, the limb weight was obtained as 1.25 kg when calculated according to [13].
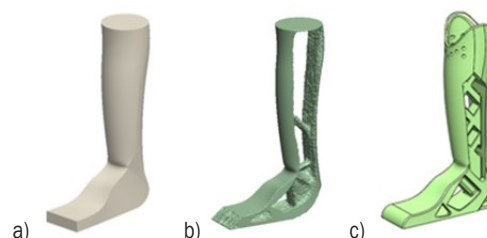

Fig. 9. *Below-knee prosthetic leg models; a) the first 3D model of the prosthetic leg below-knee, b) first optimized below-knee prosthetic leg model, and c) the final prosthetic model was modified for a support-free additive manufacturing process and a porous-socket and heel piece were added to the design*

As a result of the topology optimization analysis according to the mass response constraint method, the mass of the prosthetic model was reduced from 1.886 kg to 0.772 kg. The 59 % lighter prosthetic leg model is shown in Fig. 9b. The model was remodeled in SolidWorks software according to the optimization obtained . In order to print the 3D prosthetic model without the use of support material in 3D printing technologies such as FDM, the prosthetic model was designed according to the 45-degree rule (Fig. 9c). After obtaining the aimed prosthetic leg weight with the optimized prosthetic leg model, a socket section as shown in Fig. 9c was added for wearing the prosthetic and a heel section as shown in Fig. 9c for better balance. The designed socket section is both wearable and has sweat pores that allow air to circulate to reduce perspiration. The heel section is designed to improve better balance and ease of shoe wear. The designed socket section is both wearable and has sweat pores that allow air to circulate to reduce perspiration. The

Table 5. *Comparison of the analysis results of below-knee prosthetic leg models*

Prosthetic leg models	Weight of prosthetic leg models [kg]	The weight of prosthetic leg model as a percentage of body weight [%]	Total deformation [mm]	Von Mises stress [MPa]	Safety factor
3D First below-knee prosthetic leg model	1.886	8.57	5.739	3.207	4.08
Optimized below-knee prosthetic leg model	0.772	3.51	7.291	9.396	1.42
Final model designed for 3D printing	0.936	4.25	4.883	3.217	4.14

heel section is designed to improve balance and ease of shoe wear.

The total deformation and von Mises stress analysis results of the final below-knee prosthetic leg models optimized and designed for 3D printing are shown in Fig. 10.
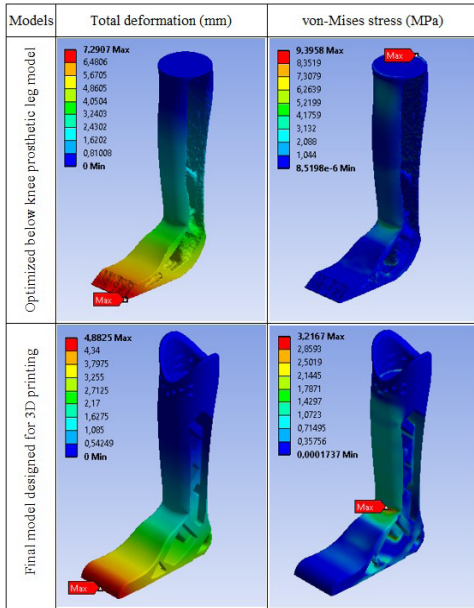

Fig. 10. *Total deformation and stress analysis results of the optimized design (first row) and the design improved for 3D printing (second row)*

2.3 Comparison of Analysis Results of Below-Knee Prosthetic Leg Models

The comparison of the structural analysis results of the below-knee prosthetic leg models is shown in Table 5. After optimization, the mass of the first 3D below-knee prosthetic leg model was reduced from 1.886 kg to 0.772 kg. With the addition of the heel and socket, the mass of the final model was 0.936 kg, corresponding to 4.25 % of the body weight. As a result, the final model designed for 3D printing was obtained with a 50.37 % reduction in the weight of the first below-knee prosthetic leg model.

According to the structural analysis results of the below-knee prosthetic leg models shown in Table 5, as a result of the topology optimization analysis using the mass response constraint method on the first model, which is well within the required safety margin overly safe with a safety factor of 4.08, the final model with a safety factor of 4.14 was obtained. It is known that products produced with traditional production have a higher specific strength than those produced by 3D printing [31]. Therefore, it was preferred that the

below-knee prosthetic leg model produced by 3D printing had a high safety factor.

2.4 3D printing of Optimized Final Knee Leg Prosthetic

The first 3D below-knee prosthetic leg model was optimized according to the results of the structural analysis and then the heel and socket parts were added to the model. The model was designed and updated according to the 45-degree rule. The aim was to achieve additive manufacturing without the need for support material. The final below-knee prosthetic leg model was then printed using the TPU filament in the FDM 3D printer according to the printing parameters in Table 3. The printed prosthetic is shown in Fig. 11. The printing time varies according to the 3D printer model.

Fig. 11. *3D printing ultimate below-knee prosthetic leg*

The final below-knee prosthetic leg model was fabricated on the Artillery Sidewinder X2 3D printer with a print time of 79 hours. Industrial 3D printers can cut print times by around half. According to production data, 358m of filament was used. The cost of a prosthetic, excluding electricity and labour, is approximately one spool of filament.

2.5 Results of Mechanical Compression Test

As a result of the finite element analyses, it was seen that the analyses in the 4th stage of the stance phase (terminal stance, 10° plantar flexion) of the gait condition were of critical importance in our study. To verify the results of these analyses, the 3D Printed below-knee prosthetic leg was performed a compression test with the same boundary conditions (terminal stance, 10° plantar flexion, force: 220N) (Fig. 12).

The compression test results for the 3D printed prosthetic leg are shown in Fig. 12. The data obtained

in Fig. 13 are compared in the table below with the results of the finite element analysis (Table 6).

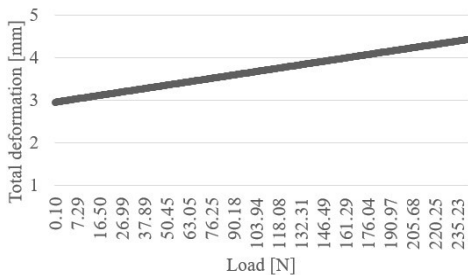**Fig. 12.** *Mechanical compression test of 3D Printed below-knee prosthetic leg*

Fig. 13. *3D printed prosthetic leg experimental total deformation results*

Table 6. *Comparison of FEM and experimental analysis results of below-knee prosthetic leg models*

Test type	Prosthetic leg models	Total deformation [mm]
FEM	Final model designed for 3D printing	4.883
Experimental	3D Printed prosthetic leg	4.307

The comparison showed a reasonable difference of 11.8 %. In additive manufacturing studies using FDM technology, there may be differences in the results obtained between mechanical analysis and FEM [32] to [34]. Because additive manufacturing is a layer-by-layer process, there is a loss of strength between layers.

3 DISCUSSION

Many lower extremity prosthetic designs have been developed to improve the quality of life by focusing on the needs of amputees [4], [10], and [35]. Amputees use the below-knee prosthetic for standing, walking, and ascending and descending stairs. They also want their prosthetics to be durable, lightweight, affordable, accessible and comfortable [2] and [35]. To demonstrate the scientific production of psychosocial and physical adaptations to amputation, Asif et al. [36] wrote an article looking at the satisfaction of prosthetic users over the last 10 years. While gender, work status and daily hours of prosthetic use influenced psychosocial adjustment, amputation level, age, education and daily prosthetic use were found to be factors that influenced physical adjustment. The area of greatest dissatisfaction with the prosthetic was weight [35]. In addition, as mentioned in the review by Ribeiro et al, lightweight prosthetics are more comfortable for people with lower limb amputations because they reduce stress on the musculoskeletal system. Heavy prosthetics can have a negative effect on patients by increasing muscle fatigue. 3D printing was shown to produce lightweight devices in most of the studies in the review [37].

In this study, we used topology optimization and additive manufacturing methods to design and manufacture a low-cost, lightweight and easily accessible prosthetic leg to improve the quality of life for below-knee amputees. Stress and deformation results obtained from finite element analyses were evaluated together. Considering the loading conditions in the gait cycle, the analysis revealed that the highest stress occurs in the terminal stance phase of compression, while the lowest stress occurs in the initial contact phase. In addition, the highest deformation for the loading conditions occurred in the terminal stance phase, while the lowest deformation occurred in the initial contact phase. Looking at the loading conditions in the stair ascent and descent cycle, it was observed that the highest stress and deformation occurred in plantar flexion during stair descent, while the lowest stress and deformation occurred in dorsal flexion during stair ascent. According to the results of the structural analyses performed for all the loading conditions examined in the situation of standing, walking, ascending and descending stairs; the highest stress occurred in the terminal stance phase of gait, while the lowest stress occurred in the initial contact phase of gait. According to the results of the FEM analysis of the prosthetic in the Rochlitz and Palmer study [14], the greatest stress was found in the ankle portion of the prosthetic. In our study it was observed that in all the FEM analysis results of standing, walking, ascending and descending stairs, the maximum stress was in the same region as reported by Rochlitz and Pammer in their study. Furthermore, the highest deformation in all loading conditions in our study occurred in plantar flexion during stair descent,

while the lowest deformation occurred in the first contact phase of walking.

A topology optimization analysis was performed for the below-knee prosthetic considering the highest tensile loading condition. The goal was to design a prosthetic that was lighter than the weight of the lower limb. In our study, we considered children with frequent prosthetic needs, and the average weight of the lower limb was determined by considering the anthropometric data of the target group [3]. Topology optimization provides the optimum distribution of the material within a predefined design space for a given load and boundary conditions. The mass reduction method identifies the areas of least stress and removes them from the design to reduce weight. Therefore, an optimum material arrangement is obtained by providing the necessary strength conditions, where a good design concept can be achieved [38]. As a result of the topology optimization analysis performed using the mass reduction method, the mass of the prosthetic model was reduced by 59 % (Fig. 9b). A porous socket section to reduce sweating and a heel section to increase stability of the prosthetic were added to the optimized model. The optimized model was remodeled using the 45-degree rule without the use of backing material (Fig. 9c). The final model was fabricated using 3D FDM technology. Support-free design provided less production time and cost.

Mechanical testing can be applied to 3D printed prosthetic components [39]. However, mechanical test results differ from FEM results due to the layer-by-layer manufacturing nature of 3D printing. Therefore, the safety factor is kept high for 3D printed parts [31]. To verify the results of the simulation analyses, a compression test was performed on the 3D printed below-knee prosthetic leg using the same boundary conditions (Fig. 12). The data obtained from the compression test and results of the simulation analysis are compared in Table 6. The comparative test showed a difference of 11.8 % from the FEM results. This difference is reasonable considering other studies applying finite element analysis (FEA) to 3D printed parts [32] and [40]. Nicoloso et al. [10] designed a below-knee prosthetic leg model separately for the socket, pylon and foot parts. After performing the structural analysis of the model, they fabricated the model as a single part using 3D printing. They provide a weight reduction of 55 % in the prosthetic. Tao et al. [4] also used the topology optimization method for their prosthetic design and provided a weight reduction of 62 % in the final design compared to the initial design. In our study, the below-knee prosthetic model includes the socket, pylon, and foot

components. The mass of the model was first reduced from 1.886 kg to 0.772 kg. After adding the heel and socket, the final model weighed 0.936 kg. Thus, the final model was achieved with a weight reduction of 50.37 %. When 3D printing method is compared with traditional casting methods, it is known that a wide variety of materials are available and that each material differs in terms of flexibility, mechanical strength and biocompatibility. However, each material has its own limitations in terms of the stresses and strains that can occur on the prosthetic device [41]. Plastic materials such as acrylonitrile butadiene styrene (ABS), polylactic acid (PLA) and TPU have been used in the fabrication of various biomedical devices by 3D printing [41] and [42]. Shamsuddin et al. [40] and Rochlitz and Pammer [14] have fabricated prosthetic feet using ABS material. Fadzil et al. [43] fabricated a socket for a prosthetic leg with PLA. However, these materials without elasticity cannot provide sufficient energy absorption. In addition, the rigidity of the structures may cause an uncomfortable experience for users. In this study, we aimed to exploit the high-strength properties of hard-TPU [16] and to provide a more comfortable experience than other thermoplastics by absorbing energy during walking through its flexibility. TPU was also preferred to provide better contact with the ground with its non-slip feature [17] and to provide ease of wear with its flexibility in the socket part. The final prosthetic leg model designed for 3D printing was printed on an FDM 3D printer fully loaded with hard TPU filament so that it could flex over reasonable ranges of displacement (Fig. 11). It was fabricated on the 3D printer with a print time of 79 hours. According to the fabrication data, 358 m of filament was consumed. Excluding electricity consumption and labour costs, the cost of a prosthetic is approximately one spool of filament. 3D printing provides several benefits for our optimized prosthetic design. Firstly, it allows for the creation of complex geometries that are difficult or impossible to achieve with traditional manufacturing methods [44]. Secondly, it enables the fabrication of our design in less time and with less waste without having to set up a production line. Not only does 3D printing use less material, but it also reduces the amount of material wasted, which contributes to a reduction in both material and production costs, as it requires less labor [45]. On the other hand, traditional custom prosthetics can be very costly for the person with an amputation. If the amputation is performed early in life, the growing child will need to be fitted with a prosthetic every few years. 3D printing has the potential to reduce costs, and a prosthetic can be printed within hours to

accommodate the growth of a young person with an amputation [46]. The prosthetic model can be easily scaled and customized for patients with different physical characteristics. Even the customized models for each patient can be made fabricated directly with 3D printing. The ease with which a 3D printed prosthetic can be scanned, designed, printed and fitted in a matter of days is beneficial in clinical practice, allowing for earlier rehabilitation and shorter hospital stays [47]. Patients are fitted with their prosthetic in less time than with traditional prostheses and can start rehabilitation earlier, preventing further deterioration and loss of muscle strength. If rehabilitation begins earlier, patients are more likely to be discharged from the hospital sooner. Many of the studies reviewed by Ribeiro et al. [37] demonstrate the speed of assembly and production processes associated with 3D printing. Thirdly, it provides the benefits of increased design freedom, including the ability to use the results of topology optimization algorithms for a lightweight design. Finally, it reduces the lifecycle time between concept, design, manufacturing and delivery of validated products [44].

In addition, additive manufacturing plays a key role in Industry 4.0 by saving time and costs, being decisive for process efficiency, and reducing its complexity, allowing for custom production and highly decentralized production processes [48]. Customers can upload their 3D designs in various file formats and receive their 3D printed parts anywhere in the world. The prosthetic design developed in our study can be fabricated on an FDM 3D printer without support material and can also be easily scaled to different sizes for different patients using any slicer software. This can facilitate global access to prosthetics by allowing prosthetics to be fabricated where the patient lives.

In this study, standing, walking, stair ascending and descending conditions were considered and the prosthetic design was developed according to the analysis performed for these conditions. However, the conditions such as running and jumping were not taken into account. In addition, this novel below-knee prosthetic leg design has not been studied in any clinical trials. In the future, clinical analyses may be performed with patients of different ages and gender.

4 CONCLUSIONS

This study aimed to design and fabricate a low-cost, lightweight, high-strength and easily accessible prosthetic leg for below-knee amputees. Therefore, a design optimization and manufacturing process were proposed and performed. The first prosthetic model was designed with anthropometric data and then the model was optimized considering load conditions of standing, walking, stair ascending and descending using the topology optimization method and FEM. In addition, the model was modified according to the 45-degree rule for a support-free design to reduce material usage, production time and post-processing. The final model was obtained by adding a porous socket for wearing and a heel section that increases stability. A total mass reduction of 50.37 % was achieved with the final model. The safety of the structure was validated by using the finite element analysis and the compression test.

The optimized prosthetic design uses less material, and combines lower cost, lightness and high strength together by reducing mass. In this way, more comfortable and lighter products can be designed for users, while also contributing to economic viability and environmental sustainability. Optimized designs are often complex in shape and may not be suitable for traditional manufacturing methods. Additive manufacturing has the ability to solve this limitation of optimized designs and enable the production of highly complex geometries. Additive manufacturing eliminates the need for production lines that include processes such as moulding, cutting, drilling, milling and heating. It also eliminates production errors caused by inexperienced operators. 3D printers use Gcode data, and it is easy to generate Gcode with this technology. Therefore, design and scale changes made in the 3D model can be quickly transferred to the manufacturing process.

The optimized below-knee prosthetic leg design and manufacturing process proposed in this study can be considered an alternative solution for people with limited access to prosthetics around the world. There are more than 40 million people world-wide who require assistive devices, including prosthetics and orthoses. Only 5 % to 15 % of those who could benefit from assistive products have access [49]. Additive manufacturing is compatible with Industry 4.0 and the online production model [20] and [50]. By sending online production instructions to a desktop 3D printer on the other side of the world, biomedical device needs can be met without shipping to regions with limited access, and supply costs can be minimized.

5 REFERENCES

[1] Khan, W., Muntimadugu, E., Jaffe, M., Domb, A.J. (2014). Implantable Medical Devices. Domb, A., Khan, W. (Eds.), Focal Controlled Drug Delivery. *Advances in Delivery Science and*

Technology, Springer, Boston, p. 33-59, **DOI:10.1007/978-1-4614 9434-8_2**.

[2] Manz, S., Valette, R., Damonte, F., Gaudio, L.A., Gonzalez-Vargas, J., Sartori, M., Dosen, S., Rietman, J. (2022). A review of user needs to drive the development of lower limb prosthetics. *Journal of NeuroEngineering and Rehabilitation*, vol. 19, 119, **DOI:10.1186/s12984-022-01097-1**.

[3] Ocak, B., Gulumser, G. (2009). Foot measurement standardization of adolescent boys in 7-14 age group. *Textiles and Clothing*, p. 157-162.

[4] Tao, Z., Ahn, H.J., Lian, C., Lee, K.H. Lee, C.H. (2017). Design and optimization of prosthetic foot by using polylactic acid 3D printing. *Journal of Mechanical Science and Technology*, vol. 31, p. 2393-2398, **DOI:10.1007/s12206-017-0436-2**.

[5] Preatoni, G., Valle, G., Petrini, F.M., Raspopovic, S. (2021). Lightening the perceived prosthetic weight with neural embodiment promoted by sensory feedback. *Current Biology*, vol. 31, no. 5, p. 1065-1071.e4, **DOI:10.1016/j.cub.2020.11.069**.

[6] Top, N., Gokce, H., Sahin, I. (2019). Topology optimization for additive manufacturing: An application on handbrake mechanism. J*ournal of Selcuk-Technic*, vol. 18, no. 1, p. 1-13.

[7] Solis, M.J.R., Ramírez, J.O.D., Salazar, J.M., Ochoa, J.A.R., Roa, A.G. (2021). Optimization of running blade prosthetics utilizing crow search algorithm assisted by artificial neural networks, *Strojniški vestnik - Journal of Mechanical Engineering*, vol. 67, no. 3, p. 88-100, **DOI:10.5545/sv-jme.2020.6990**.

[8] Dickinson, A.S., Steer, J.W., Worsley, P.R. (2017). Finite element analysis of the amputated lower limb: A systematic review and recommendations. *Medical Engineering & Physics*, vol. 43, p. 1-18, **DOI:10.1016/j.medengphy.2017.02.008**.

[9] Vijayan, V., Kumar, S.A., Gautham, S., Masthan, M.M., Piraichudan, N. (2021). Design and analysis of prosthetic foot using additive manufacturing technique. *Materials Today: Proceedings*, vol. 37, 1665-1671, **DOI:10.1016/j.matpr.2020.07.195**.

[10] Nicoloso, L.D.V., Pelz, J., Barrack, H., Kuester, F. (2021). Towards 3D printing of a monocoque transtibial prosthetic using a bio-inspired design workflow. *Rapid Prototyping Journal*, vol. 27, no. 11, p. 67-80, **DOI:10.1108/RPJ-06-2021-0136**.

[11] Chethan, K.H. Zuber, M., Bhat, S.N., Shenoy, S.S., Kini, C.R. (2019). Static structural analysis of different stem designs used in total hip arthroplasty using finite element method. *Heliyon*, vol. 5, no. 6, e01767, **DOI:10.1016/j.heliyon.2019.e01767**.

[12] Chethan, K.H., Zuber, M., Bhat, S.N., Shenoy, S.B. (2020). Optimized trapezoidal-shaped hip implant for total hip arthroplasty using finite element analysis. *Cogent Engineering*, vol. 7, no. 1, **DOI:10.1080/23311916.2020.1719575**.

[13] de Leva, P. (1996). Adjustments to Zatsiorsky-Seluyanov's segment inertia parameters. *Journal of Biomechanics*, vol. 29, no. 9, 1223-1230, **DOI:10.1016/0021-290(95)00178-6**.

[14] Rochlitz, B., Pammer, D. (2017). Design and analysis of 3D printable foot prosthetic. *Periodica Polytechnica Mechanical Engineering*, vol. 61, no. 4, p. 282-287, **DOI:10.3311/PPme.11085**.

[15] Merola, M., Affatato, S. (2019). Materials for hip prostheses: A review of wear and loading considerations. *Materials*, vol. 12, no. 3, 495, **DOI:10.3390/ma12030495**.

[16] Ahmed, M.H., Jamshid, A., Amjad, U., Azhar, A., ul Hassan, M.Z., Tiwana, M.I., Qureshi, W.S., Alanazi, E. (2022). 3D printable thermoplastic polyurethane energy efficient passive foot. *3D Printing and Additive Manufacturing*, vol. 9, no. 6, **DOI:10.1089/3dp.2021.0022**.

[17] Hättig, J., Wenz, E., Lauter, M., Möller, P. (2009). An economical way to produce high-end interiors. *ATZProduktion Worldwide*, vol. 2, p. 4-7, **DOI:10.1007/BF03224182**.

[18] Dizon, J.R.C., Espera, A.H.Jr. , Chen, Q., Advincula, R.C. (2018). Mechanical characterization of 3D-printed polymers. *Additive Manufacturing*, vol. 20, p. 44-67, **DOI:10.1016/j.addma.2017.12.002**.

[19] Kozior, T., Mamun, A., Trabelsi, M., Sabantina, L., Ehrmann, A. (2020). Quality of the surface texture and mechanical properties of FDM printed samples after thermal and chemical treatment. *Strojniški vestnik - Journal of Mechanical Engineering*, vol. 66, no. 2, p. 105-113, **DOI:10.5545/sv-jme.2019.6322**.

[20] Surmen, H K. (2019). Additive manufacturing (3D printing): Technologies and applications. *Uludag University Journal of The Faculty of Engineering*, vol. 24, no. 2, p. 373-392.

[21] Prathyusha, A.L.R., Babu, G.R. (2022). A review on additive manufacturing and topology optimization process for weight reduction studies in various industrial applications. *Materials Today: Proceedings*, vol. 62, p. 109-117, **DOI:10.1016/j.matpr.2022.02.604**.

[22] Gulcimen, B., Ulku, S. (2008). The Investigation of human foot biomechanics. Uludag University Journal of The Faculty of Engineering, vol. 13, no. 2, p. 27-33.

[23] Tuval, M., Yahalom, A. (2014). Newton's Third Law in the Framework of Special Relativity. *The European Physical Journal Plus*, vol. 129, 240, **DOI:10.1140/epjp/i2014-142 40-x**.

[24] Houglum, P.A. (2010). *Therapeutic Exercise for Musculoskeletal Injuries*, 3rd ed., Human Kinetics, Champaign.

[25] Whittle, M. (2014). *Gait Analysis: An Introduction*, Butterworth-Heinemann, Oxford.

[26] Protopapadaki, A., Drechsler, W.I., Cramp, M.C., Coutts, F.J., Scott, O.M. (2007). Hip, knee, ankle kinematics and kinetics during stair ascent and descent in healthy young individuals. *Clinical Biomechanics*, vol. 22, no. 2, p. 203-210., **DOI:10.1016/j.clinbiomech.2006.09.010**.

[27] Silverman, A.K., Neptune, R.R., Sinitski, E.H., Wilken, J.M. (2014). Whole-body angular momentum during stair ascent and descent. *Gait & Posture*, vol. 39, no. 4, p. 1109-1114, **DOI:10.1016/j.gaitpost.2014.01.025**.

[28] ASTM International, Designation: D638 - 14, (2015). *Standard Test Method for Tensile Properties of Plastics*. Agencies of the U.S. Department of Defense, Washington.

[29] Potok, B. (2018). Weighing in on lighter vs. heavier prosthetic legs, from *https://amputeestore.com/ blogs/amputee-life/ weighing-in-on-lighter -vs-heavier-prosthetic-legs*, accessed on 2024-10-11.

[30] Gao, T., Zhang, W. (2011). A mass constraint formulation for structural topology optimization with multiphase materials.

International Journal for Numerical Methods in Engineering, vol. 88, no. 8, p. 774-796, **DOI: 10.1002/nme.3197**.

[31] Carneiro, O.S., Silva, A.F., Gomes, R. (2015). Fused deposition modeling with polypropylene. *Materials & Design*, vol. 83, p. 768-776, **DOI:10.1016/j.matdes.2015.06.053**.

[32] Szabó, D. (2019). Linear elastic finite element investigation of titanium specimen produced by additive manufacturing. *International Journal of Engineering and Management Sciences*, vol. 4, no. 4, p. 85-91, **DOI:10.21791/IJEMS.2019.4.9**.

[33] Pepelnjak, T., Karimi, A., Maček, A., Mole, N. (2020). Altering the elastic properties of 3D Printed poly-lactic acid (PLA) parts by compressive cyclic loading. *Materials*, vol. 13, no. 19, 4456, **DOI:10.3390/ma13194456**.

[34] Karimi, A., Mole, N., Pepelnjak, T. (2022). Numerical Investigation of the cycling loading behavior of 3D-printed poly-lactic acid (PLA) cylindrical lightweight samples during compression testing. *Applied Sciences*, vol. 12, no. 16, 8018, **DOI:10.3390/app12168018**.

[35] Abbady, H.E.M.A., Klinkenberg, E.T.M., de Moel, L., Nicolai, N., van der Stelt, M., Verhulst, A.C., Maal, T.J.J., Brouwers, L. (2022). 3D-printed prostheses in developing countries: A systematic review. *Prosthetics and Orthotics International*, vol. 46, no. 1, p. 19-30, **DOI:10.1097/pxr.00000000 00000057**.

[36] Asif, M., Tiwana, M. I., Khan, U. S., Qureshi, W. S., Iqbal, J., Rashid, N., & Naseer, N. (2021). Advancements, trends and future prospects of lower limb prosthesis. *IEEE Access*, vol. 9, 85956-85977, **DOI:10.1109/ACCESS.2021.3086807**.

[37] Ribeiro, D., Cimino, S.R., Mayo, A.L., Ratto, M., Hitzig, S.L. (2021). 3D printing and amputation: a scoping review. *Disability and Rehabilitation: Assistive Technology*, vol. 16, no. 2, p. 221-240, **DOI:10.1080/17483107.2019.1646825**.

[38] Glamsch, J., Deese, K., Rieg, F. (2019). Methods for increased efficiency of FEM-based topology optimization. *International Journal of Simulation Modelling*, vol. 18, no. 3, p. 453-463, **DOI:10.2507/IJSIMM18(3)482**.

[39] Nickel, E.A., Barrons, K.J., Owen, M.K., Hand, B.D., Hansen, A.H., Desjardins, J.D. (2020). Strength testing of definitive transtibial prosthetic sockets made using 3D-printing technology. *Journal of Prosthetics and Orthotics*, vol. 32, no. 4, p. 295-300, **DOI:10.1097/JPO.0000000000000294**.

[40] Shamsuddin, S., Rafie, M.E.E., Ahmad, I.F., Zulkifli, W.Z., Ali, M.M., Amir, A. (2023). Design and development of printable prosthetic foot using acrylonitrile butadiene styrene (ABS) for below knee amputation (BKA). *Malaysian Journal on Composites Science and Manufacturing*, vol. 10, no. 1, p. 11-23, **DOI:10.37934/mjcsm.10.1.1123**.

[41] Djukanović, M., Damjanovic, M., Radunovic, L., Jovanovic, M. (2022). Optimisation of PLA filament consumption for 3D printing using the annealing method in home environment. *Strojniški vestnik - Journal of Mechanical Engineering*, vol. 68, no. 3, p. 185-190, **DOI:10.5545/sv-jme.2021.7426**.

[42] Bacak, S. (2022). Investigation of the tensile strength properties of samples produced using different parameters from ABS, PLA, TPU (Flex) materials. *Süleyman Demirel University, Journal of Yekarum*, vol. 7, no. 2, p. 58-64.

[43] Fadzil, W.F.A.W., Mazlan, M.A., Abdullah, A.H. (2020). Effects of infill density on 3D printed socket for transtibial prosthetic leg. *Journal of Mechanical Engineering*, vol. SI 9, no. 1, p. 229-238.

[44] Zadpoor, A.A. (2017). Design for additive bio-manufacturing: from patient-specific medical devices to rationally designed meta-biomaterials. *International Journal of Molecular Sciences*, vol. 18, no. 8, 1607, **DOI:10.3390/ijms18081607**.

[45] Ferreira, N.V., Leal, N., Correia Sa, I., Reis, A., Marques, M. (2014) Computer-aided method and rapid prototyping for the personalized fabrication of a silicone bandage digital prosthesis. *Acta Medica Portuguesa*, vol. 27, no. 6, p. 775-779, **DOI:10.20344/amp.5308**.

[46] Zuniga, J., Katsavelis, D., Peck, J., Stollberg, J., Petrykowski, M., Carson, A., Fernandez, C. (2015). Cyborg beast: a low-cost 3D-printed prosthetic hand for children with upper-limb differences. *BMC Research Notes*, vol. 8, no. 10, **DOI:10.1186/s 13104-015-0971-9**.

[47] Imanishi, J., Choong, P.F.M. (2015). Three-dimensional printed calcaneal prosthesis following total calcanectomy. *International Journal of Surgery Case Report*, vol. 10, p. 83-87, **DOI:10.1016/j.ijscr.2015.02.037**.

[48] Horst, D.J., Duvoisin, C.A., Vieira, R.D.A. (2018). Additive manufacturing at Industry 4.0: a review. *International Journal of Engineering and Technical Research*, vol. 8, no. 8, p. 3-8.

[49] World Health Organization (2017). Standards for Prosthetics and Orthotics, Part 1: Standards, from *https://iris.who.int/bitstream/handle/10665/259209/9789241512480-part1-eng.pdf*, accessed on 2024-10-11.

[50] Chong, S., Pan, G.T., Chin, J., Show, P.L., Yang, T.C.K., Huang, C.M. (2018). Integration of 3D printing and industry 4.0 into engineering teaching. *Sustainability*, vol. 10, no. 11, **DOI:10.3390/su10113960**.